Available online at www.qu.edu.iq/journalcm
JOURNAL OF AL-QADISIYAH FOR COMPUTER SCIENCE AND MATHEMATICS
ISSN:2521-3504(online) ISSN:2074-0204(print)

Influence of a Rotating Frame on the Peristaltic Flow of a Rabinowitsch Fluid Model in an Inclined Channel

Saba S. Hasen [a,b] **,** ***Ahmed M. Abdulhadi*** [a]

[a]*Department of Mathematics, College of Science,,University of Baghdad , Baghdad, Iraq. Email: sabaoday79@gmail.com , ahm6161@yahoo.com*

[b]*Department of Applied Science, University of Technology, Baghdad, Iraq. Email: sabaoday79@gmail.com*

ARTICLE INFO

Article history:
Received: 18 /12/2019
Rrevised form: 25 /12/2019
Accepted : 28 /01/2020
Available online: 18 /02/2020

Keywords:

Peristaltic flow, Rabinowitsch fluid, rotating frame ,Heat transfer , inclined channel.

ABSTRACT

The article deals with the simultaneous existence of inclination and rotation on the peristaltic activity of the Rabinowitsch fluid model on a symmetric inclined channel. The heat transfer analysis and heat source/sink are taken into consideration. The governing equations are addressed using the low -Reynolds and infinite wave approximations. The system of ordinary differential equations is obtained from nonlinear partial differential equations and solved numerically. The axial velocity, secondary velocity, temperature field, and stream function were calculated and analyzed. The influences of the physical parameters are discussed graphically, and the study revealed that the rotation enhances the axial velocity, secondary velocity, and temperature field.

MSC..

DOI : 10.29304/jqcm.2020.12.1.661

1. Introduction

Today, interest in peristalsis issues has increased due to many applications in physics and medicine. The relaxation and contraction mechanism in the fluid movement along the wall is known as peristaltic motion. Peristalsis is important in many physiological processes, such as the urine transmission to the bladder through the ureter, the action of bile in the gallbladder, fluid movement through lymphatic vessels, spermatozoa movement in ducts, and movement of the esophagus when swallowing food. Peristalsis is also important in many industrial applications as pumps to transport of many kinds of fluid, radar systems, micro-pumps in pharmacology and fuel control in the rocket chamber, and power generators. Several studies have been presented about peristaltic flow [1, 2, 3].

∗Corresponding author : Saba S. Hasen

Email addresses: : sabaoday79@gmail.com

Communicated by 'Alaa H. H. Al-Ka'bi'

Non-Newtonian fluids are currently of great interest because of their many uses in science and technology. Several models have been used to describe rheological behavior in non-Newtonian fluids, including the Rabinowitsch model in which has been important for understanding the rheological behavior of biological fluids. This model is characterized by its cubic stress relationship, and displays the properties of shear-thinning or pseudo-plastic (the pseudo-plasticity coefficient ζ is positive, e.g., blood plasma and ketchup), shear-thickening or Dilatant (ζ is negative, e.g., sand and polyethylene glycol), Newtonian (ζ is zero e.g., air and water) models. Several researchers have studied this model. (Vaidya et al. 2019)[4] studied a Rabinowitsch fluid under the influence of variable liquid properties and a compliant wall. (Manjunatha et al. 2.19)[5] examined the peristaltic flow of a Rabinowitsch fluid through a non-uniform inclined channel in two dimensions. (Lin 2012)[6] discussed a theoretical study of the Rabinowitsch model's influence on the squeeze film properties through parallel annular disks. Other authors [7,8,9] illustrated engineering applications of Rabinowitsch fluids.

Numerous studies deal with the effect of heat transfer because of its importance in fluid mechanics as illustrated in industrial fields and mechanical engineering and physiological operations, such as food treatment biochemical processes, transfer in polymers, biomedical engineering, oxygenation, hemodialysis and promulgation of chemical impurities. The investigations about the heat transfer influences have been reported in [10, 11,12].

The rotation phenomenon has vast applications in cosmic and geophysical flows and helps us to better comprehend galaxy formation and ocean circulation. Rotational diffusion accounts for nanoparticle orientation in fluids. The following is a review of studies that discuss the effects of rotation. (Hayat et al. 2016) [13] present the effect of MHD on the peristaltic flow of a Jeffrey fluid through a rotating channel. (Hayat et al. 2017) [14] introduced the effect of heat transfer on the peristaltic flow of Ree-Eyring fluids in the rotating frame. (Dar et al. 2016) [15] discussed the effects of rotation and inclined magnetic field on the peristaltic transpose of a micro polar fluid through an inclined symmetric channel (Abd- Alla et al. 2015)[16] discussed the influence of MHD on the peristaltic flow of a Jeffrey fluid through an asymmetric rotating channel.(Padma et al. 2018) [17] presented the Hall influence and MHD flow on the unsteady flow between two parallel plates through a rotating porous media channel. (Hatami et al. 2018) [18] used analytical methods to solve the three-dimensional problem of a Nano-fluid film on an inclined rotating disk. There have also been other attempts to study the effect of rotation [19,20, 21].

This article helps to understand and study the influence of rotation phenomena as well as the effect of heat transfer on the peristaltic motion of the Rabinowitsch fluid model through a uniform channel characterized as symmetrical and inclined. For further clarification, this article organized to Section 2 that presents the physical modeling statement for our problem. The system of non-linear equations has been solved numerically and the results of the axial velocity, secondary velocity, temperature, and stream function are interpreted for relevant parameters and analyzed through graphs in Section 3. Finally, conclusions are given in Section 4.

2. Modeling

The paper examines an incompressible Rabinowitsch fluid model in peristaltic motion through a uniform, inclined and rotating channel, such that the model and channel rotate with uniform angular velocity Ω about the horizontal axis (see Fig.1). The non-Newtonian fluid (Rabinowitsch fluid) fills a three-dimensional symmetric channel of width 2a, and the flow of the fluid, induced by the sinusoidal wave trains of wavelength λ and constant speed c, propagate along the channel borders, b represent the wave amplitude and $\bar{t}$ the wave time. The geometrical equation of the wall surface can be expressed as:

$$\bar{Z} = \bar{H}(\bar{X}, \bar{t}) = a + b \sin\frac{2\pi}{\lambda}(\bar{X} - c\bar{t}) \quad (1)$$

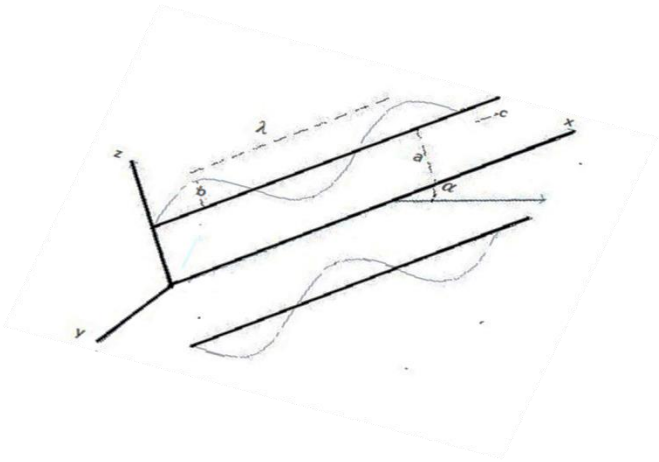

Fig. 1. Geometry of the problem

Governing equations of three dimensional for incompressible fluid flow in the laboratory frame is given by

$$\nabla\vec{V} = 0 \tag{2}$$

$$\rho\left[\frac{\partial\vec{V}}{\partial\bar{t}} + (\vec{V}.\nabla)\vec{V}\right] + \rho\left[\Omega \times (\Omega \times \vec{V}) + 2\Omega \times \vec{V}\right] = \nabla\bar{\tau} + \rho g \tag{3}$$

$$\rho C_p \frac{dT}{dt} = \kappa\,\nabla^2 T + \bar{\tau}.\vec{L} + Q_0(T - T_0) \tag{4}$$

where $\vec{V} = (\bar{U}, \bar{V}, \bar{W})$ is the fluid velocity, ρ is the fluid density, $\vec{\Omega} = (0,0,\Omega) = \Omega\,\vec{k}$ is the rotation vector ($\vec{k}$ is a unit vector), $\bar{\tau}$ denotes the Cauchy stress tensor, $\vec{L}$ is the gradient operator, C_p is the specific heat, κ is thermal conductivity of the fluid, T is temperature, and Q_0 denotes the heat source/sink parameter. In Eq. 3, the centrifugal force $\rho\vec{\Omega} \wedge (\vec{\Omega} \wedge \vec{V})$ and the Coriolis force $2\rho(\vec{\Omega} \wedge \vec{V})$ are two additional describing motion in the rotating frame.

Rewrite Eqs. (2) -(4) as

$$\frac{\partial\bar{U}}{\partial\bar{X}} + \frac{\partial\bar{V}}{\partial\bar{Y}} + \frac{\partial\bar{W}}{\partial\bar{Z}} = 0 \tag{5}$$

$$\rho\left(\frac{\partial\bar{U}}{\partial\bar{t}} + \bar{U}\frac{\partial\bar{U}}{\partial\bar{X}} + \bar{V}\frac{\partial\bar{U}}{\partial\bar{Y}} + \bar{W}\frac{\partial\bar{U}}{\partial\bar{Z}}\right) - 2\rho\Omega\bar{V} = -\frac{\partial\bar{P}}{\partial\bar{X}} + \frac{\partial\bar{S}_{\bar{X}\bar{X}}}{\partial\bar{X}} + \frac{\partial\bar{S}_{\bar{X}\bar{Y}}}{\partial\bar{Y}} + \frac{\partial\bar{S}_{\bar{X}\bar{Z}}}{\partial\bar{Z}} + \rho g\sin\alpha \tag{6}$$

$$\rho\left(\frac{\partial\bar{V}}{\partial\bar{t}} + \bar{U}\frac{\partial\bar{V}}{\partial\bar{X}} + \bar{V}\frac{\partial\bar{V}}{\partial\bar{Y}} + \bar{W}\frac{\partial\bar{V}}{\partial\bar{Z}}\right) + 2\rho\Omega\bar{U} = -\frac{\partial\bar{P}}{\partial\bar{Y}} + \frac{\partial\bar{S}_{\bar{Y}\bar{X}}}{\partial\bar{X}} + \frac{\partial\bar{S}_{\bar{Y}\bar{Y}}}{\partial\bar{Y}} + \frac{\partial\bar{S}_{\bar{Y}\bar{Z}}}{\partial\bar{Z}} \tag{7}$$

$$\rho\left(\frac{\partial\bar{W}}{\partial\bar{t}} + \bar{U}\frac{\partial\bar{W}}{\partial\bar{X}} + \bar{V}\frac{\partial\bar{W}}{\partial\bar{Y}} + \bar{W}\frac{\partial\bar{W}}{\partial\bar{Z}}\right) = -\frac{\partial\bar{P}}{\partial\bar{Z}} + \frac{\partial\bar{S}_{\bar{Z}\bar{X}}}{\partial\bar{X}} + \frac{\partial\bar{S}_{\bar{Z}\bar{Y}}}{\partial\bar{Y}} + \frac{\partial\bar{S}_{\bar{Z}\bar{Z}}}{\partial\bar{Z}} - \rho g\cos\alpha \tag{8}$$

$$\rho C_p\left(\frac{\partial T}{\partial\bar{t}} + \bar{U}\frac{\partial T}{\partial\bar{X}} + \bar{V}\frac{\partial T}{\partial\bar{Y}} + \bar{W}\frac{\partial T}{\partial\bar{Z}}\right) = \kappa\left(\frac{\partial^2 T}{\partial\bar{X}^2} + \frac{\partial^2 T}{\partial\bar{Y}^2} + \frac{\partial^2 T}{\partial\bar{Z}^2}\right) + \bar{S}_{\bar{X}\bar{X}}\frac{\partial\bar{U}}{\partial\bar{X}} + \bar{S}_{\bar{X}\bar{Z}}\left(\frac{\partial\bar{U}}{\partial\bar{Z}} + \frac{\partial\bar{W}}{\partial\bar{X}}\right) + \bar{S}_{\bar{Z}\bar{Z}}\frac{\partial\bar{W}}{\partial\bar{Z}} + Q_0(T - T_0) \tag{9}$$

The constituent equation for the Rabinowitsch fluid model is expressed as follows:

$$\bar{S}_{\bar{X}\bar{Z}} + \bar{\zeta}\,\bar{S}^3_{\bar{X}\bar{Z}} = \mu\frac{\partial\bar{U}}{\partial\bar{Z}} \tag{10}$$

$$\bar{S}_{\bar{Y}\bar{Z}} + \bar{\zeta}\,\bar{S}^3_{\bar{Y}\bar{Z}} = \mu\frac{\partial\bar{V}}{\partial\bar{Z}} \tag{11}$$

The associated boundary conditions are no-slip conditions at the walls of the channel

$$\frac{\partial\bar{U}}{\partial\bar{Z}} = 0, \quad \frac{\partial\bar{V}}{\partial\bar{Z}} = 0, \quad \kappa\frac{\partial T}{\partial\bar{Z}} = 0 \quad at \quad \bar{Z} = 0 \tag{12}$$

$$\bar{U} = 0, \quad \bar{V} = 0, \quad \kappa \frac{\partial T}{\partial \bar{Z}} = -\bar{H}_1 (T_0 - T) \quad at \quad \bar{Z} = \bar{H} \tag{13}$$

where $\bar{U}, \bar{V}$ and $\bar{W}$ are the velocity components in the $\bar{X}, \bar{Y}$ and $\bar{Z}$ directions respectively, $\bar{P}$($\bar{P} = \tilde{P} - \frac{1}{2}\bar{R}^2\Omega^2\rho$) is the modified pressure, $\bar{R}$ is given by $\bar{R}^2 = \bar{X}^2 + \bar{Y}^2$, μ is the fluid viscosity and $\bar{\zeta}$ refers to the coefficient of pseudo-plasticity.

The steady flow is obtained when we move away from the laboratory(unsteady) frame of reference $(\bar{X}, \bar{Y}, \bar{Z})$ to the wave (steady) frame of reference $(\bar{x}, \bar{y}, \bar{z})$ with constant wave propagation speed. The transformation between two frames is given by

$$\bar{x} = \bar{X} - c\bar{t} \quad , \bar{y} = \bar{Y} \ , \bar{z} = \bar{Z} \quad , \bar{u} = \bar{U} - c \quad , \bar{v} = \bar{V} \quad , \bar{w} = \overline{W} \quad , \ \bar{p} = \bar{P} \tag{14}$$

Using Eq. (14), Eqs. (5)- (9) become

$$\frac{\partial \bar{u}}{\partial \bar{x}} + \frac{\partial \bar{v}}{\partial \bar{y}} + \frac{\partial \bar{w}}{\partial \bar{z}} = 0 \tag{15}$$

$$\rho\left((\bar{u} + c)\frac{\partial \bar{u}}{\partial \bar{x}} + \bar{v}\frac{\partial \bar{u}}{\partial \bar{y}} + \bar{w}\frac{\partial \bar{u}}{\partial \bar{z}}\right) - 2\rho\Omega\bar{v} = -\frac{\partial \bar{p}}{\partial \bar{x}} + \frac{\partial \bar{S}_{\bar{x}\bar{x}}}{\partial x} + \frac{\partial \bar{S}_{\bar{y}\bar{y}}}{\partial \bar{y}} + \frac{\partial \bar{S}_{\bar{x}\bar{z}}}{\partial \bar{z}} + \rho g \sin\alpha \tag{16}$$

$$\rho\left((\bar{u} + c)\frac{\partial \bar{v}}{\partial \bar{x}} + \bar{v}\frac{\partial \bar{v}}{\partial \bar{y}} + \bar{w}\frac{\partial \bar{v}}{\partial \bar{z}}\right) + 2\rho\Omega(\bar{u} + c) = -\frac{\partial \bar{p}}{\partial \bar{y}} + \frac{\partial \bar{S}_{\bar{y}\bar{x}}}{\partial \bar{x}} + \frac{\partial \bar{S}_{\bar{y}\bar{y}}}{\partial \bar{y}} + \frac{\partial \bar{S}_{\bar{y}\bar{z}}}{\partial \bar{z}} \tag{17}$$

$$\rho\left((\bar{u} + c)\frac{\partial \bar{w}}{\partial \bar{x}} + \bar{v}\frac{\partial \bar{w}}{\partial \bar{y}} + \bar{w}\frac{\partial \bar{w}}{\partial \bar{z}}\right) = -\frac{\partial \bar{p}}{\partial \bar{z}} + \frac{\partial \bar{S}_{\bar{z}\bar{x}}}{\partial \bar{x}} + \frac{\partial \bar{S}_{\bar{z}\bar{y}}}{\partial \bar{y}} + \frac{\partial \bar{S}_{\bar{z}\bar{z}}}{\partial \bar{z}} - \rho g \cos\alpha \tag{18}$$

$$\rho C_p\left((\bar{u} + c)\frac{\partial T}{\partial \bar{x}} + \bar{v}\frac{\partial T}{\partial \bar{y}} + \bar{w}\frac{\partial T}{\partial \bar{z}}\right) = \kappa\left(\frac{\partial^2 T}{\partial \bar{x}^2} + \frac{\partial^2 T}{\partial \bar{y}^2} + \frac{\partial^2 T}{\partial \bar{z}^2}\right) + \bar{S}_{\bar{x}\bar{x}}\frac{\partial \bar{u}+c}{\partial \bar{x}} + \bar{S}_{\bar{x}\bar{z}}\left(\frac{\partial \bar{u}+c}{\partial \bar{z}} + \frac{\partial \bar{w}}{\partial \bar{x}}\right) + \bar{S}_{\bar{z}\bar{z}}\frac{\partial \bar{w}}{\partial \bar{z}} + Q_0(T - T_0) \tag{19}$$

The non-dimensional quantities can be introduced as follows:

$$x = \frac{\bar{x}}{\lambda}, \quad y = \frac{\bar{y}}{\lambda}, \quad z = \frac{\bar{z}}{a}, \quad t = \frac{c\bar{t}}{\lambda}, \quad p = \frac{a^2\bar{p}}{c\mu\lambda}, \ \delta = \frac{a}{\lambda} \ , \ u = \frac{\bar{u}}{c}, \quad v = \frac{\bar{v}}{c}, \quad w = \frac{\bar{w}}{c}, \quad Re = \frac{\rho c a}{\mu},$$
$$S_{ij} = \frac{a\bar{S}_{ij}}{c\mu} \ , \theta = \frac{T - T_0}{T_0}, T' = \frac{Re\Omega a}{c}, \ \eta = \frac{Q_0 a^2}{\kappa}, \ B_r = \frac{c^2\mu}{\kappa T_0}, \ B_i = \frac{ah}{\kappa},$$
$$F = \frac{c\mu}{\rho g a^2}, \ \zeta = \frac{c^2\mu^2\bar{\zeta}}{a^2} \ , u = \psi_z \ , \ w = -\delta\psi_x \tag{20}$$

To proceed, we employ Eqs. (14) and (20) in Eqs. (10), (11) and (15) -(19), yielding

$$\frac{c}{\lambda}\frac{\partial u}{\partial x} + \frac{c}{\lambda}\frac{\partial v}{\partial y} + \frac{c}{a}\frac{\partial w}{\partial z} = 0 \tag{21}$$

$$\rho\left(c(u+1)\frac{\partial cu}{\partial \lambda x} + cv\frac{\partial cu}{\partial \lambda y} + cw\frac{\partial cu}{\partial az}\right) - 2\rho\frac{\mathrm{c}T'}{Re\ a}\mathrm{c\ v} = -\frac{\partial c\mu\lambda p}{a^2\partial\lambda x} + \frac{\partial c\mu S_{xx}}{a\partial\lambda x} + \frac{\partial c\mu S_{xy}}{a\partial\lambda y} + \frac{\partial c\mu S_{xz}}{a\partial az} + \rho\frac{c\mu}{\rho F a^2}\sin\alpha \tag{22}$$

$$\rho\left(c(u+1)\frac{\partial cv}{\partial \lambda x} + cv\frac{\partial cv}{\partial \lambda y} + cw\frac{\partial cv}{\partial az}\right) - 2\rho\frac{\mathrm{c}T'}{Re\ a}\mathrm{c\ (u+1)} = -\frac{\partial c\mu\lambda p}{a^2\partial\lambda y} + \frac{\partial c\mu S_{yx}}{a\partial\lambda x} + \frac{\partial c\mu S_{yy}}{a\partial\lambda y} + \frac{\partial c\mu S_{yz}}{a\partial az} \tag{23}$$

$$\rho\left(c(u+1)\frac{\partial cw}{\partial \lambda x} + cv\frac{\partial cw}{\partial \lambda y} + cw\frac{\partial cw}{\partial az}\right) = -\frac{\partial c\mu\lambda p}{a^2\partial az} + \frac{\partial c\mu S_{zx}}{a\partial\lambda x} + \frac{\partial c\mu S_{zy}}{a\partial\lambda y} + \frac{\partial c\mu S_{zz}}{a\partial az} + \rho\frac{c\mu}{\rho F a^2}\cos\alpha \tag{24}$$

$$\rho C_p\left(c(u+1)\frac{\partial(\theta T_0 - T_0)}{\partial\lambda x} + cv\frac{\partial(\theta T_0 - T_0)}{\partial\lambda y} + cw\frac{\partial(\theta T_0 - T_0)}{\partial az}\right) = \kappa\left(\frac{\partial^2(\theta T_0 - T_0)}{\partial(\lambda x)^2} + \frac{\partial^2(\theta T_0 - T_0)}{\partial(\lambda y)^2} + \frac{\partial^2(\theta T_0 - T_0)}{\partial(az)^2}\right) + \frac{c\mu S_{xx}}{a}\frac{\partial cu}{\partial\lambda x} + \frac{c\mu S_{xz}}{a}\left(\frac{\partial cu}{\partial az} + \frac{\partial cw}{\partial\lambda x}\right) + \frac{c\mu S_{zz}}{a}\frac{\partial cw}{\partial az} + \frac{\kappa\,\eta}{a^2}(\theta T_0 - T_0) \tag{25}$$

$$\frac{c\,\mu\,S_{xz}}{a} + \frac{a^2\zeta}{c^2\mu^2}\,\frac{c^3\mu^3 s_{xz}^3}{a^3} = \mu\frac{\partial cu}{\partial az} \tag{26}$$

$$\frac{c\mu S_{yz}}{a} + \frac{a^2\zeta}{c^2\mu^2}\,\frac{c^3\,\mu^3\,S_{yz}^3}{a^3} = \mu\frac{\partial cv}{\partial az} \tag{27}$$

After some simplification and using the assumption of infinite wavelength and low Reynolds number, the problem becomes

$$-2\mathrm{T}'\mathrm{v} = -\frac{\partial p}{\partial x} + \frac{\partial S_{xz}}{\partial z} + \frac{\sin\alpha}{F} \tag{28}$$

$$-2\mathrm{T}'\,(\mathrm{u}+1) = -\frac{\partial p}{\partial y} + \frac{\partial S_{yz}}{\partial z} \tag{29}$$

$$\frac{\partial p}{\partial z} = 0 \tag{30}$$

$$\frac{\partial^2\theta}{\partial z^2} + B_r S_{xz}\frac{\partial u}{\partial z} + \eta\,\theta = 0 \tag{31}$$

$$S_{xz} + \zeta\,S_{xz}^3 = \frac{\partial u}{\partial z} \tag{32}$$

$$S_{yz} + \zeta\,S_{yz}^3 = \frac{\partial v}{\partial z} \tag{33}$$

The non-dimensional conditions are

$$\psi = 0 \quad,\ \psi_{zz} = 0,\ v_z = 0,\ u_z = 0,\ S_{xz} = 0,\ S_{yz} = 0,\ \frac{\partial\theta}{\partial z} = 0 \qquad at\ \ z = 0 \tag{34}$$

$$\psi = F_1 \quad,\ v = 0, \quad u = -1, \qquad \frac{\partial\theta}{\partial z} - B_i\theta = 0 \qquad at\ \ z = h \tag{35}$$

$$h = 1 + \epsilon\sin 2\pi x \tag{36}$$

where ψ is the stream function, T' is the Taylor number, F is the body force, and the Brinkman number B_r, α is the angle of inclination, η is the heat source /sink parameter, B_i is the Biot number and F_1 is calculated from the following

$$F_1 = \int_0^h u\,dz \tag{37}$$

The pressure term $\frac{\partial \mathrm{p}}{\partial \mathrm{y}}$ in Eq. (29) will be neglected due to secondary flow which results from the effect of the rotation.

3. Numerical solution and Discussion

This section reviews the numerical results of velocity, temperature and stream function graphically. A numerical technique is employed to solve the system of nonlinear equations (28) -(33) with boundary conditions equations (34) -(36) since the exact solution is difficult to obtain. The solution is built on (ND Solve) command with Mathematica programing. The pressure gradient in Eq. (28) is taken as a constant to facilitate the numerical solution.

3.1. The axial velocity u:

Figure 2 elucidates the impact of the fluid parameters T', ζ, F, α on the axial velocity u. Figure 2(a) characterizes the role of T' on the axial velocity. In the middle of the channel, the velocity is higher, whereas, at the boundary, the velocity decreases when the value of the T' is large. Figure 2(b) illustrates that, with dilatant nature, the velocity of the fluid is maximum but is minimum with pseudo-plastic nature. Figure 2(c) indicates the influence of F on the

velocity: the velocity increases at the wall when F increases while the reverse occurs at the center of the channel. Figure 2(d) shows that the axial velocity is enhanced in the middle whenever the α increases.

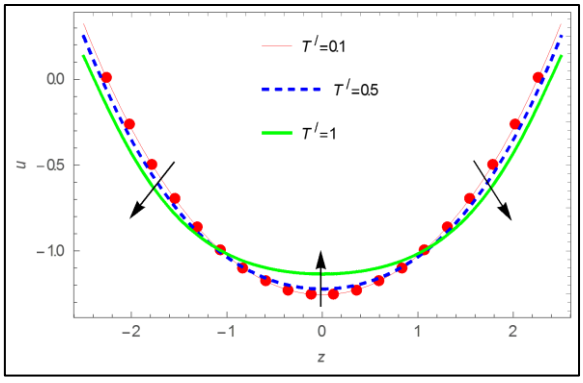

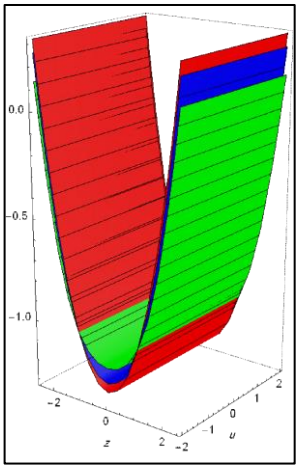

Fig.2 (a)

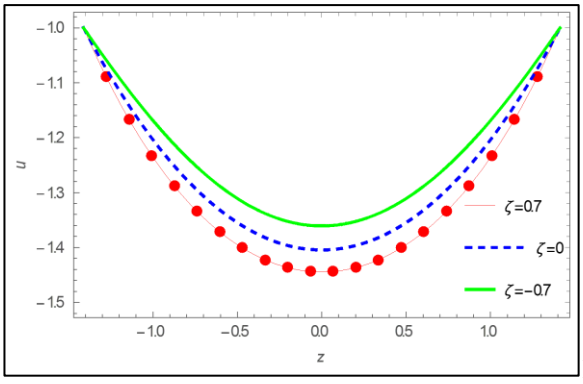

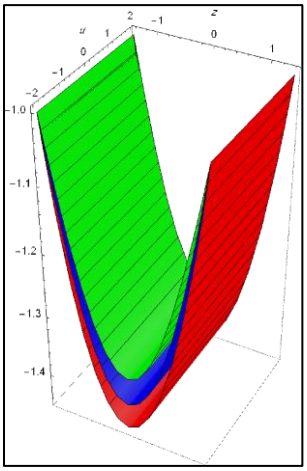

Fig.2 (b)

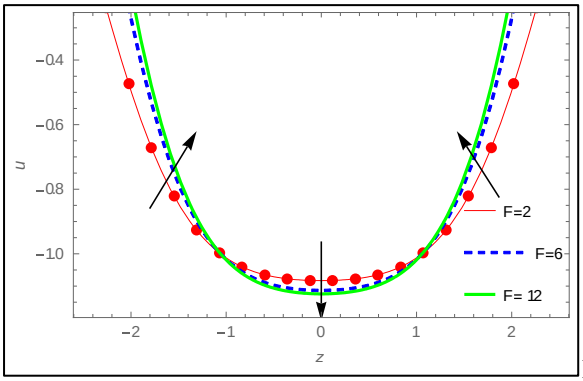

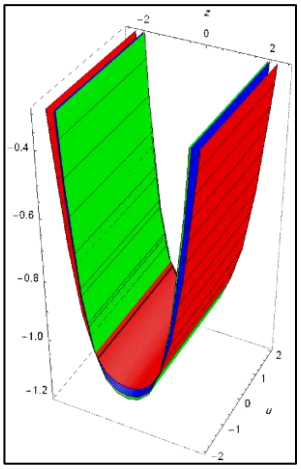

Fig.2 (c)

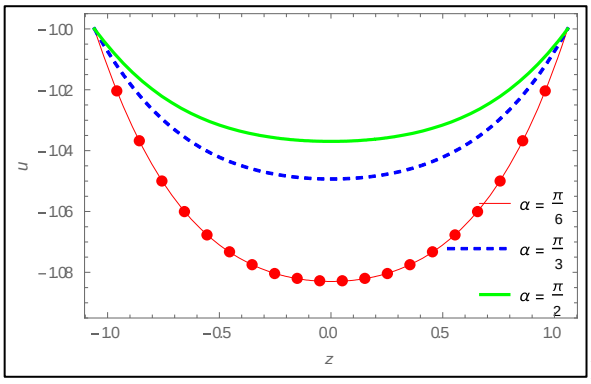

Fig.2 (d)

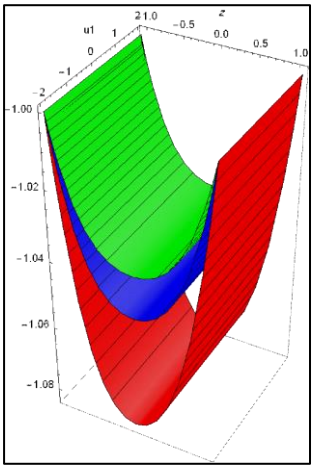

Fig. 2. axial velocity profiles u for various values of Fig. 2(a) Taylor number T′, Fig.2 (b) the coefficient of Pseudo-plasticity ζ. Fig.2 (c) the body force F. Fig.2 (d) the angle of inclination α, and other parameters are $(\frac{dp}{dx} = 0.7, \epsilon = 0.1, x = 0.1, B_i = 2, B_r = 0.5, S = 0.4)$.

3.2. Secondary Velocity v:

Figure (3) shows the effectiveness of parameters T', ζ, F and α on the secondary velocity v. Figure 3(a) illustrates that rotation enhances the secondary velocity at the centerline and reduces it near the wall. Figure 3(b) shows that the secondary velocity is maximum with the pseudo-plastic fluid, slows down with the Newtonian fluid and becomes a minimum in the dilatant fluid. Figure 3(c) demonstrates that the secondary velocity is augmented when F increases. The influence of α on the secondary flow is shown in Figure 3(d), where v decreases when α increases.

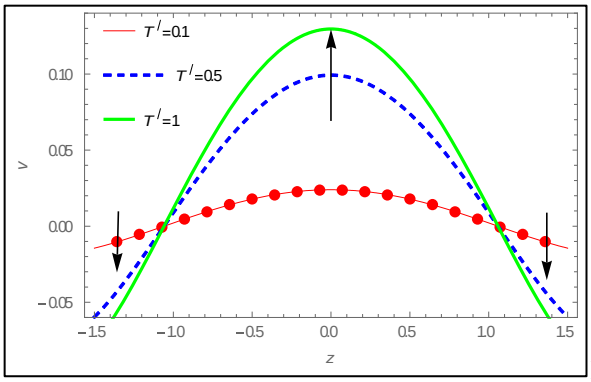

Fig.3 (a)

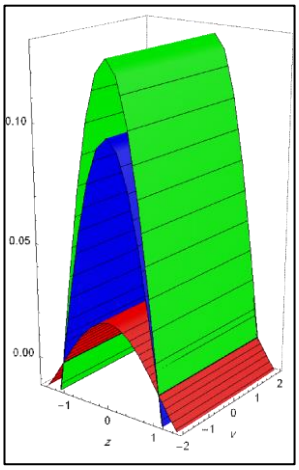

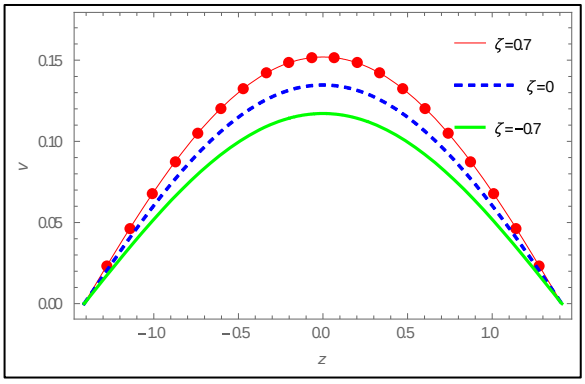

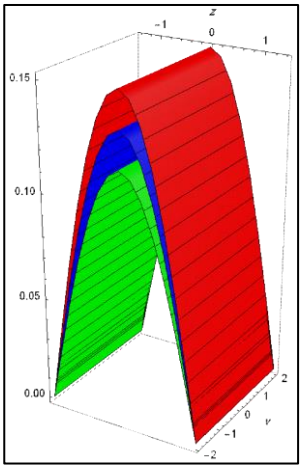

Fig.3 (b)

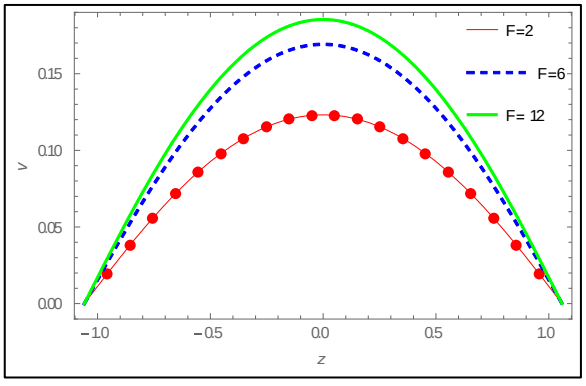

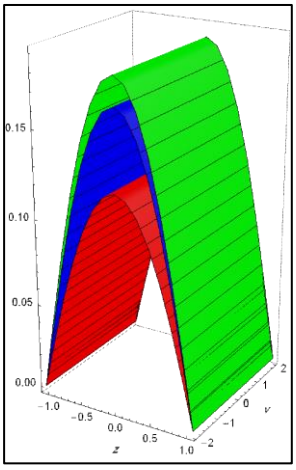

Fig.3 (c)

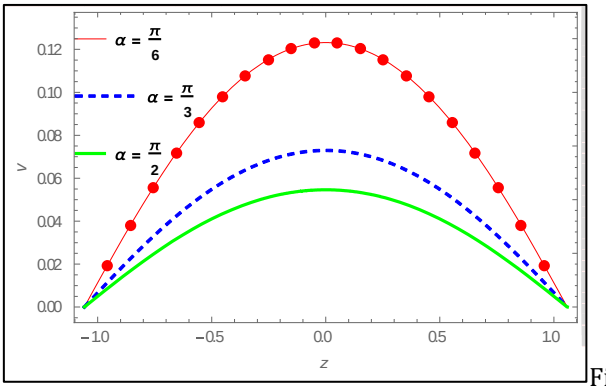

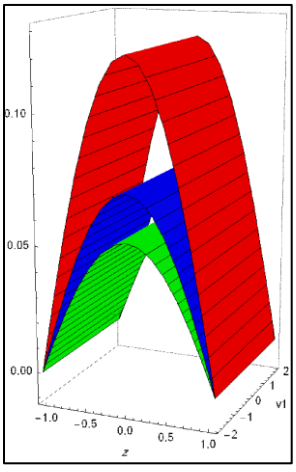

Fig.3 (d)

Fig. 3. Secondary velocity profiles v for various values of Fig.3(a) Taylor number T', Fig.3 (b) the coefficient of Pseudo-plasticity ζ. Fig.3 (c) the body force F . Fig.3 (d) the angle of inclination α, and other parameters are $(\frac{dp}{dx} = 0.7, \epsilon = 0.1, x = 0.1,\ B_i = 2,\ B_r = 0.5\ , S = 0.4)$.

3.3. Temperature profile θ:

Figure 4 disclose the effectiveness of different parameters on the temperature θ. Figure 4(a) examines the behavior of the temperature θ with T' (Taylor number). We observe that θ increases with increasing T'. When comparing the temperature of the three classes of fluid, we notice that the dilatant fluid temperature is the highest, while the pseudo-plastic fluid is the lowest and the Newtonian fluid takes the mean level see Figure 4(b). In Figure 4(c) the

temperature is enhanced when B_i (Biot number) increases. It is clear from Figure 4(d) that θ diminishes with increasing F. Fig.4 (e) demonstrates that whenever α expands, the θ increases. In Figure 4(f), we observe increasing η results in a temperature decrease in the middle of the channel and an increase near the wall. Figure 4(g) shows that θ decreases when the magnitude B_r increases.

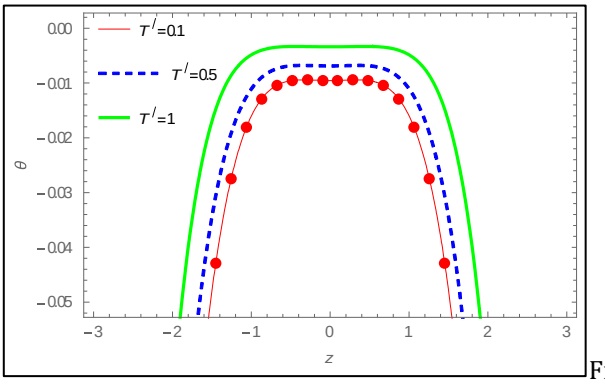

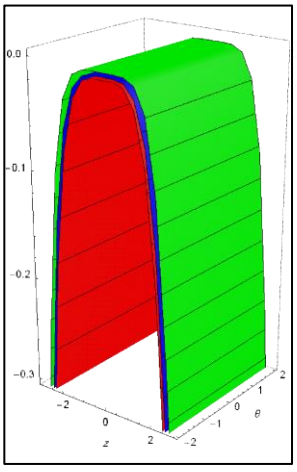

Fig.4 (a)

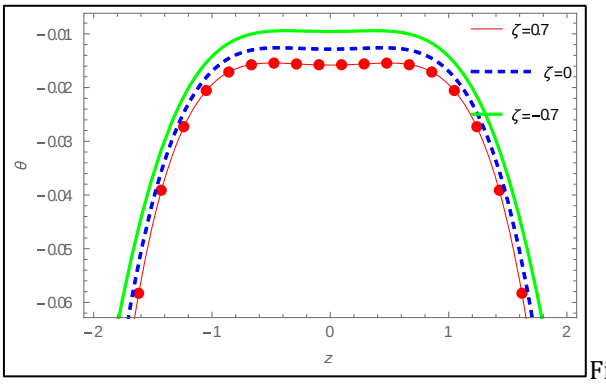

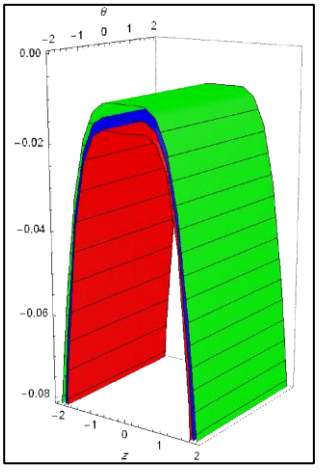

Fig.4 (b)

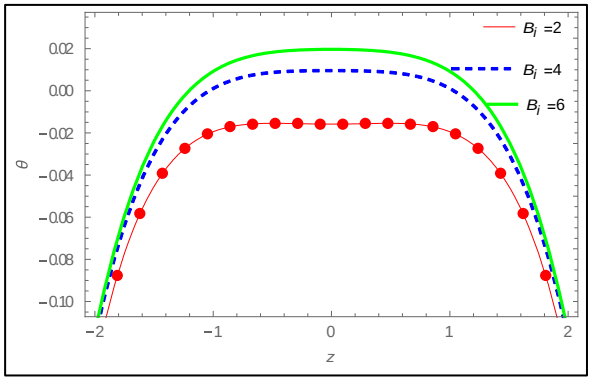

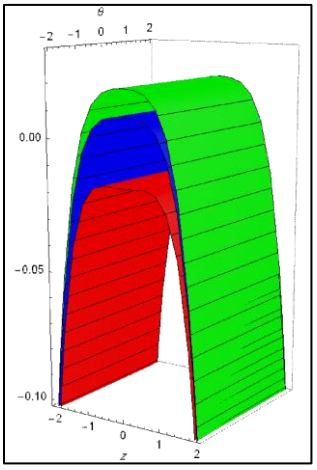

Fig.4 (c)

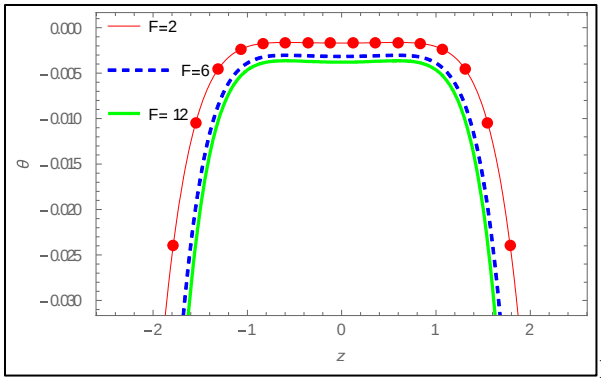

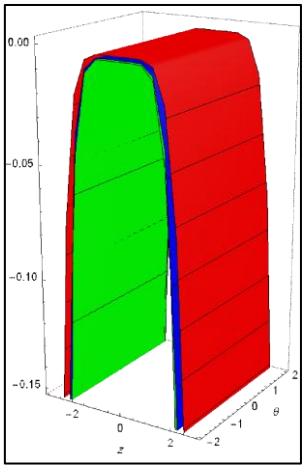

Fig.4 (d)

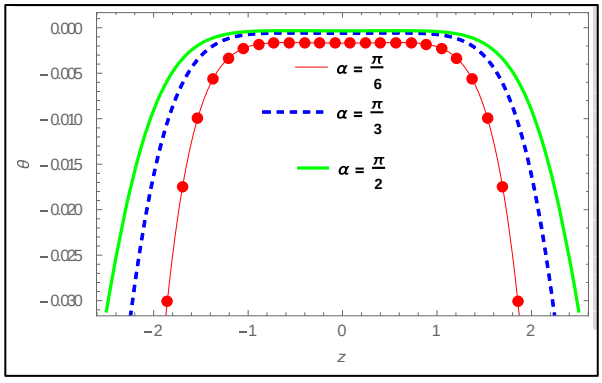

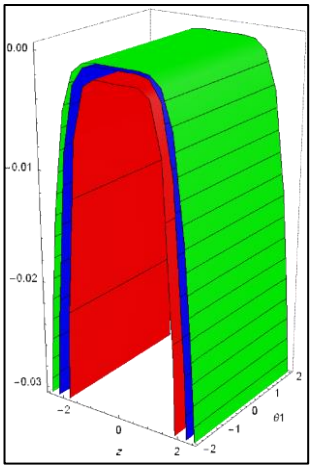

Fig.4 (e)

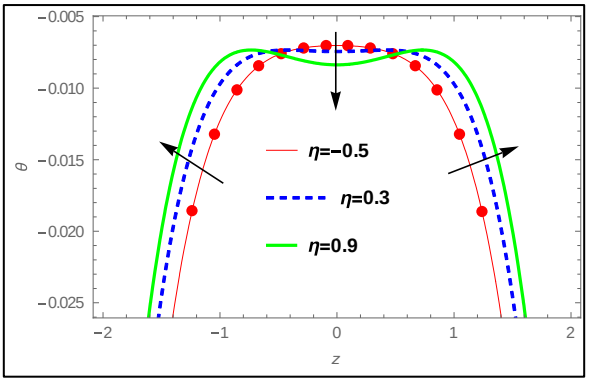

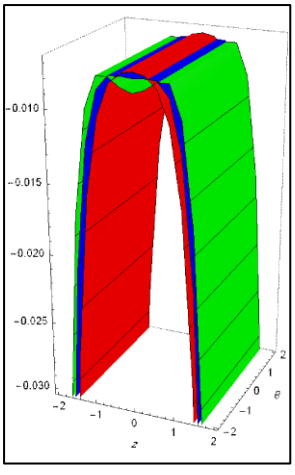

Fig.4 (f)

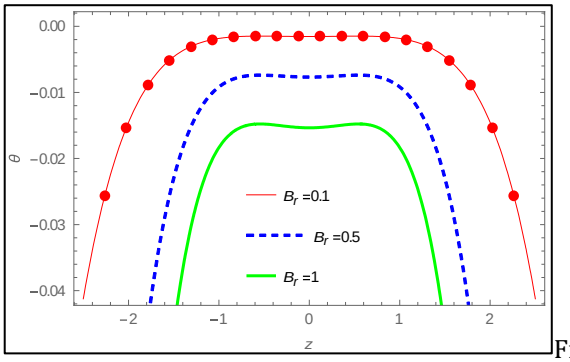

Fig.4 (g)

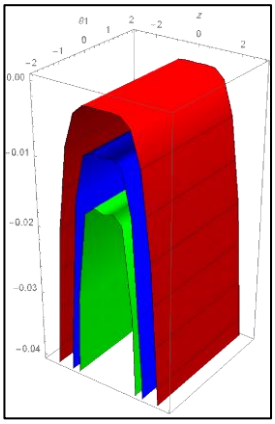

Fig. 4. Temperature profiles θ for various values of Fig.4 (a) Taylor number T', Fig.4 (b) the coefficient of Pseudo-plasticity ζ .Fig.4 (c) Biot number B_i .Fig.4 (d) the body force F. Fig.4 (e) the angle of inclination α, Fig.4(f) the heat source/ sink η and Fig.4 (g) the Brinkman number B_r and other parameters are $(\frac{dp}{dx} = 0.7, \epsilon = 0.1, x = 0.1)$.

3.4. Stream Function ψ:

Figure 5 examine the behavior that the stream function takes when the value of the physical parameters varies. It is clear from the graphs that the stream function only has non zero values in a bounded region of space and has wavy conduct at the z-axis. Figure 5(a) illustrates the effect of T'on the stream ψ and shows that the stream increases initially and then gradually decreases. Figure 5(b) demonstrates that the stream function is maximal for a pseudo-plastic fluid, decreases for a Newtonian fluid and becomes minimal for a dilatant fluid. As shown in Figure 5(c), the stream function increasing with increasing F. Figure 5(d) shows that ψ decreases with increasing α.

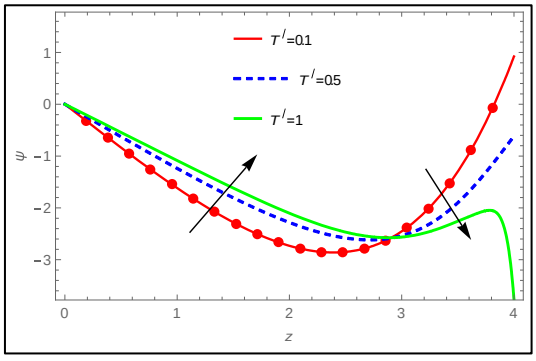

Fig.5 (a)

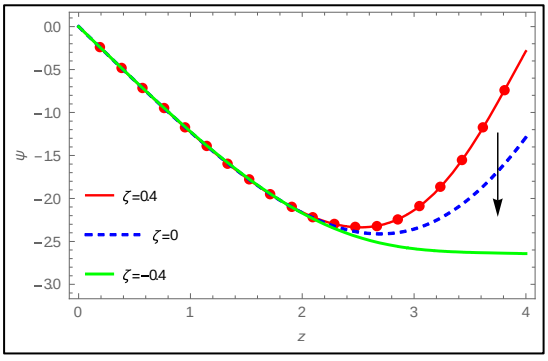

Fig.5 (b)

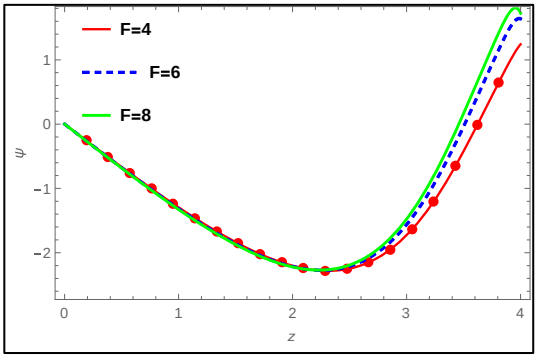

Fig.5 (c)

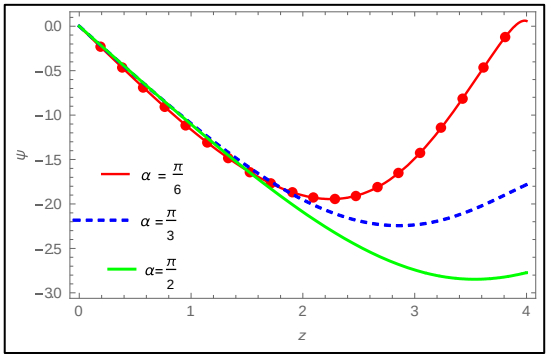

Fig.5 (d)

Fig. 5. Stream function profiles ψ for various values of Fig.5 (a) Taylor number T', Fig.5 (b) the coefficient of Pseudo-plasticity ζ, Fig.5 (c) the body force F, Fig.5 (d) the angle of inclination α, and other parameters are $(\frac{dp}{dx} = 0.7, \epsilon = 0.7, x = 0.2, B_i = 2, B_r = 0.5, S = 0.4)$.

4. Conclusions

We study the peristaltic transport of a Rabinowitsch fluid under no-slip conditions, in three-dimensional fluid flow. The present study clarifies the impact of rotation, inclined channel and source/sink on the Rabinowitsch fluid. We list the main observations below:

- The impact of rotation on the axial and secondary velocity is the same, such that the velocity increases in the middle of the channel and decreases near the wall.
- The inclination and the rotation of the channel raise the temperature of the fluid.
- Initially, the stream function increases with the rotating the channel and then gradually decreases.
- The axial velocity improves with the inclination of the channel, but the opposite occurs for the secondary velocity.
- The stream function decreases when the angle of the inclination increases, and increases when the body force F increases.
- The presence of F and B_r decrease the temperature of the fluid.
- The presence of B_i raises the temperature of the fluid.
- The temperature decreases in the middle of the channel and increases near the wall with the presence of a heat source/sink S
- F enhances the axial velocity near the wall but decreases it at the center of the channel.
- The secondary velocity increases with the presence of F.

REFERENCES

[1] V. Jagadeesh, S. Sreenadh, P. Lakshminarayana, "Influence of Inclined Magnetic Field on the Peristaltic Flow of a Jeffery fluid in an Inclined Porous Channel", *International Journal of Engineering &Technology*,(2018), 7(4.10),319-322.

[2] H. A. Ali, Ahmed M. Abdulhadi," the Peristaltic Transport of MHD Powell- Eyring Fluid through Porous Medium in Asymmetric Channel with Slip Condition", *International Journal of Science and Research*, 6,12 (2016).

[3] H. A. Ali, Ahmed M. Abdulhadi," the Peristaltic Transport of MHD Eyring- Powell Fluid Through Porous Medium in a Three Dimensional Rectangular duct", *International Journal of Pure and Applied Mathematics*, 119,18 (2018).

[4] H. Vaidya, C. Rajashekhar, G. Manjunatha, K.V. Prasad, "Peristaltic Mechanism of a Rabinowitsch Fluid in an Inclined Channel with Complaint Wall and variable Liquid Properties*", Journal of the Brazilian Society of Mechanical Sciences and Engineering*, (2019), p:41-52.

[5] G. Manjunatha, C. Rajashekhar, Hanumes Vaidya. K.V. Prasad, O.D. Makinde," Effects Wall Properties on Peristaltic Transport of Rabinowitsch Fluid Through an Inclined Non-Uniform Slippery Tube", *Defect and Diffusion Forum*,392, (2019),p:138-157.

[6] J.-Ren Lin," Non-Newtonian Squeeze Film Characteristics between Parallel Annular Disks: Rabinowitsch Fluid Model", *Tribology International* ,52,(2012),p:190-194.

[7] N.B. Naduvinamani, M. Rajashekar, A.K. Kadadi," Squeeze Film Lubrication Between Circular Stepped Plates", *Tribology International*, 73,(2014),p:,78-82.

[8] H. Vaidy, C. Rajashekhar, G. Manjunatha, K.V. Prasad," Effect of variable Liquid Properties on Peristaltic Transport of Rabinowitsch Liquid in Convectively Heated Complaint Porous Channel*", J. Cent. South Univ*. 26,(2019) , p:1116-1132.

[9] J.Lin, Li -Ming Chu, Tzu-Chen Hung, Pin- Yu Wang," Derivation of Two-Dimensional Non-Newtonian Reynolds Equation and Application to Power-Law Film Slider Bearings: Rabinowitsch Fluid Model", *Applied Mathematical Modelling,* 40,(2016),p:8832-8841.

[10] H. A. Ali, Ahmed M. Abdulhadi," Analysis of Heat Transfer on Peristaltic Transport of Powell-Eyring Fluid in an Inclined Tapered Symmetric Channel with Hall and Ohm's Heating Influences", *Journal of al-Qadisiyah for Computer Science and Mathematics*, 10,2,(2018).

[11] R. M.G.," Heat and Mass Transfer on Magneto Hydrodynamic Peristaltic Flow in a Porous Medium with Partial Slip", *Alexandria Engineering Journal*, 55,(2016),p:1225-1234.

[12] M. R. Salman, Ahmed M. Abdulhadi," Analysis of Heat and Mass Transfer in a Tapered ASymmetric Channel During Peristaltic Transport of (Pseudo plastic Nano Fluid) with variable Viscosity Under the Effect of (MHD) *", Journal of al-Qadisiyah for Computer Science and Mathematics*, 10,3,(2018),p:80-96.

[13] T. Hayat, Maimona Rafiq. Bashir Ahmad," Soret and Dufour Effects on MHD Peristaltic Flow of Jeffery Fluid in a Rotating System with Porous Medium", *PLOS one*, (2016).

[14] T. Hayat, H. Zahir, A. Alsaedi.b. Ahmad," Heat Transfer Analysis on Peristaltic Transport of Ree- Eyring Fluid in Rotating Frame", *Chinese Journal of Physics*, 55,(2017),p:1894-1907.

[15] A. Ahmad Dar, K. Elangovan," Influence of an Inclined Magnetic Field and Rotation on the Peristaltic Flow of a Micropolar Fluid in an Inclined Channel", *Hindawi Publishing Corporation (New Journal of Science)*, (2016), 14 pages.

[16] A. M. Abd- Alla, S. M. Abo-Dahab," Magnetic field and Rotation Effects on Peristaltic Transport of Jeffery fluid in an Asymmetric Channel", *Journal of Magnetism and Magnetic Materials,*374, (2015),p:680-689.

[17] G. Padma, S.V. Suneetha," Hall Effect on MHD flow through Porous Medium in a Rotating Parallel Plate Channel", *Internal Journal of Applied Engineering Research*, 13, no. 11,(2018),p:9772-9789.

[18] M. Hatami D. Jing Majeed A. Yousif," Three-Dimensional Analysis of Condensation Nanofluid Film on an Inclined Rotating Disk by Efficient Analytical Methods", *Arab Journal of Basic and Applied Sciences*, 25 no.11,(2018),p:28-73.

[19] B. Zohra, and Mohamed Najib Bouaziz." MHD Rotating Fluid Past a Semi-Infinite Vertical Moving Plate:Coriolis Force and Wall Velocity Effects" *Journal of Advanced Research in Fluid Mechanics and Thermal Sciences* 60, Issue 1 (2019),p:38-51

[20] A.M. Abd- Alla, S. M. Abo-Dahab, H.D. El- shahrany," Effects of Rotation and Magnetic Field on the Nonlinear Peristaltic Flow of second-order Fluid an ASymmetric Channel Through a Porous Medium", *Chin Phys. b,* 22,7,(2013).

[21] D.RY, Cao BY, "Superthigh-Speed Unidirectional Rotation of a Carbon Nanotube in a Sheared Fluid and its Decoupled Dynamics", *Rsc Adv*, 5,(2015),p:19-24.